Characterization of ethane jet from sub-critical to super-critical conditions through visible light and X-ray imaging

Nathalie Vallée, Guillaume Ribert, Jean-Bernard Blaisot, S. Dozias

Characterization of ethane jet from sub-critical to super-critical conditions through visible light and X-ray imaging

N. Vallée*, G. Ribert*,*, J.-B. Blaisot*, E. Robert†, S. Dozias†

*CORIA - CNRS, Normandie Université, INSA de Rouen Normandie
76000 Rouen, France

†GREMI - CNRS, Université d'Orléans, 45000 Orléans

Abstract

The injection of fuel in a high-pressure gaseous environment, for automotive, aeronautical or rocket applications leads to thermodynamic conditions where pressure exceeds the critical pressure of working fluids and thus, the supercritical state of matter is reached. Providing reliable experimental results under these particular conditions is still nowadays a challenge, but it is of great importance for the validation of numerical codes. Indeed, at such a high pressure, the distinction between gaseous and liquid phases becomes blurred as surface tension decreases and the interface disappears completely. For such special conditions, experimental data are scarce and need to be consolidated. As an example, the modification of the local refractive index induced by density gradient makes the visible-light imaging technique to be used with care. The REFINE testbench (Real-gas Effect on Fluid Injection: a Numerical and Experimental study) has been designed at CORIA Lab to study the non-reactive injection of Ethane and Propane under sub- and supercritical conditions. The ambient gas pressure can be raised up to 6 MPa and warmed up to 573 K to scan sub- and trans-critical injection conditions. The chamber is equipped with two perpendicular accesses allowing different simultaneous diagnostics to be applied to the jet. Experimental data are collected from shadowgraph, diffused backlight illumination techniques and X-Ray. Quantitative measurements of jet spreading angle, breakup length and density maps are compared to literature results.

Introduction

The study of high pressure injection is a major topic of research in the transport industry (cars, aircrafts, rockets) because it conditions the combustion performance and therefore the formation of pollutants. Under certain conditions of pressure and temperature the liquid injected into the chamber does not behave as usual and the atomization process is replaced by a diffusion one [1, 2]. The experimental study of this transition is a challenge because it requires the development of a robust, precise and well-controlled experiment as well as adapted diagnostics. The number of experiments dealing with supercritical injection is therefore small and the amount of experimental data that can be used for modeling validation [3, 4, 5] is all the more scarce [6]. In particular, the high ambient pressure locally affects the refractive index gradient making the use of laser-based diagnostics questionable [7, 6] to provide quantitative local experimental data. Nevertheless, classical diagnostics such as shadowgraphy or schlieren techniques have been used up to now to observe the transition from a system composed of distinct liquid and gaseous phases [6, 8, 9] to a system where dense and light fluids mix together because the surface tension and the heat of vaporization diminish [10, 11]. Under supercritical conditions, a dense and dark core is visible at the injector exit on shadowgraph [12] and the analysis of the spreading angle shows that supercritical jet has a behavior closer to a gaseous jet than to a liquid jet [13, 14].

In this study, the first results coming from the research program REFINE (Real-gas Effect on Fluid Injection: a Numerical and Experimental study) are provided. It consists in an injection of Ethane into an environment of Nitrogen or Helium at high pressure and moderate temperature. The objective is to deliver a set of quantitative data for the dark core length and the spreading angle of a non-assisted jet, from subcritical to supercritical pressure with respect to the liquid injected, and for various levels of ambiant temperature. A tentative to deliver the value of density on the jet axis through the radiography of the liquid jet is also presented. Radiography is an X-ray imaging technique that has been used for the study of diesel jets [15, 16] or cryogenic injections under supercritical considerations [17]. The physical principle of radiography is the absorption of X-rays by the dense fluid. The transmission of X-rays thus depends on the mixture composition, i.e. the injected fluid and its surrounding. An advantage of X-ray absorption technique is that X-rays are not subject to deflection due to optical index gradients, contrary to laser-based techniques, and the attenuation of the transmitted light is proportional to the mass of fluid crossed by the X-ray beam.

*Corresponding author: guillaume.ribert@coria.fr

Experimental setup

REFINE testbench

The experiment has been designed to study the injection and atomization of a non-assisted jet under high pressures conditions. REFINE is equipped with a steel chamber able to withstand pressures up to 10 MPa and moderate temperatures (573 K). Two optical accesses through circular silica windows of diameter 120 mm are available for simultaneous measurements (see Fig. 1). The chosen working fluids are Ethane (C_2H_6, $T_c = 305.3$ K and $p_c = 4.87$ MPa) and Propane (C_3H_8, $T_c = 369.8$ K and $p_c = 4.25$ MPa). Their moderate critical pressure and temperature are within the range of operating conditions achievable in the chamber. A one-liter pump supplies the working fluid at the liquid-gas equilibrium pressure. Before injection, the pump is filled up, and then the fluid contained inside the vessel of the pump is compressed to the target pressure plus 0.05 MPa to prevent the ambient fluid in the main chamber from entering the pump and creating an effervescent jet.

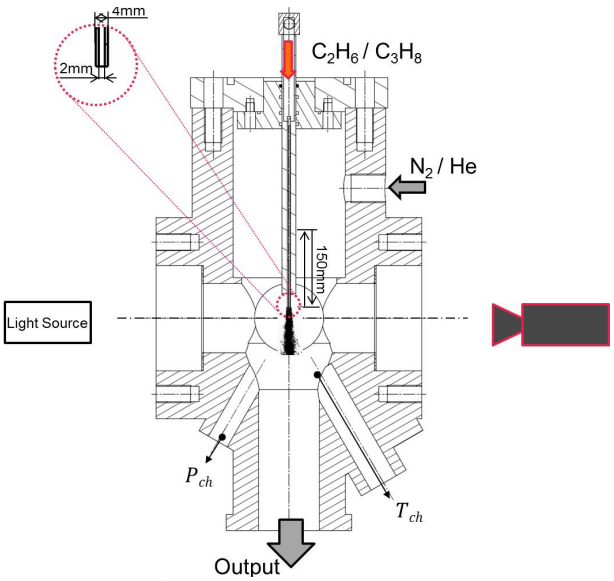

Figure 1: REFINE testbench.

The injection is performed with a sharp-edged stainless steel tube of 210 mm long, with a 4 mm outer diameter and a 2 mm inner diameter. The injector can be moved vertically over a 150 mm stroke by a motorized system located on the top of the chamber, to expand the field of view. The rig is fully instrumented with thermocouples, pressure gauges and mass flow meters. The chamber is filled with Nitrogen or Helium and the pressure is controlled with a pressure regulator having a precision of ± 0.1 MPa. To warm up the ambient fluid, two MICA heating plates are placed at the bottom of the chamber and a heater is inserted just before the feeding of N_2 ($T_c = 126.2$ K and $p_c = 3.4$ MPa) or He ($T_c = 5.2$ K and $p_c = 0.228$ MPa).

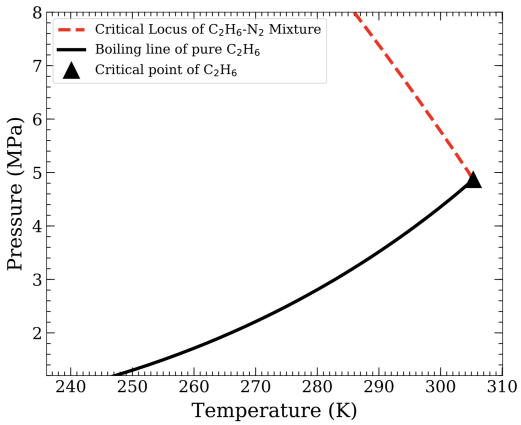

Figure 2: Caption.

Finally, the locus of critical points according to the experimental conditions encountered in the experiment

REFINE is given in Fig. 2.

Shadowgraphy

Two optical diagnostics, diffused back-light illumination (DBI) and shadowgraphy, are used to quantify the injection and atomization of the working fluids. The main difference between these two techniques lies in the light source arrangement. For shadowgraphy, a collimated laser diode (Cavitar) is used whereas a stroboscope flashlamp (MVS-2601) with a glass diffuser is used for DBI. Depending on the situation and on the desired information, different camera configurations were used, as indicated in Tab. 1. The DBI detects the largest density gradients, which are essentially located at the liquid-gas interface, and the shadowgraphy detects smoother density gradient that may be found in whole chamber.

Table 1: Table of the different configurations of camera and light source with the associate designation code used in this manuscript.

Code	Camera	Resolution (px/mm)	Field (mm)	Light
BG1	BlueCougar-x24	27.0	59.3 × 44.5	DBI
BG2-1	BlueCougar-x25a	53.5	45.8 × 38.1	DBI
BG2-2	BlueCougar-x25a	130.5	18.8 × 15.7	Shadowgraphy
PCO-1	PCO Edge 5.5	58.0	44.1 × 37.2	DBI
PCO-2	PCO Edge 5.5	121.5	294.3 × 17.8	DBI

Radiography

The production of X-rays is carried out by an X-ray generator consisting of a high-voltage generator which supplies an X-ray tube. The electrons are produced by heating the metallic filament of the cathode of the generator, before being accelerated by an electric field in a vacuum tube and hitting a metal target, the anode (or anti-cathode). A continuous radiation called Bremsstrahlung [18] is then produced. The effective radiation is the sum of the Bremsstrahlung and the fluorescence of the anode. For a copper anode, the radiation by fluorescence has an energy of about 8 keV. The electrical intensity which passes through the filament determines the quantity of electrons

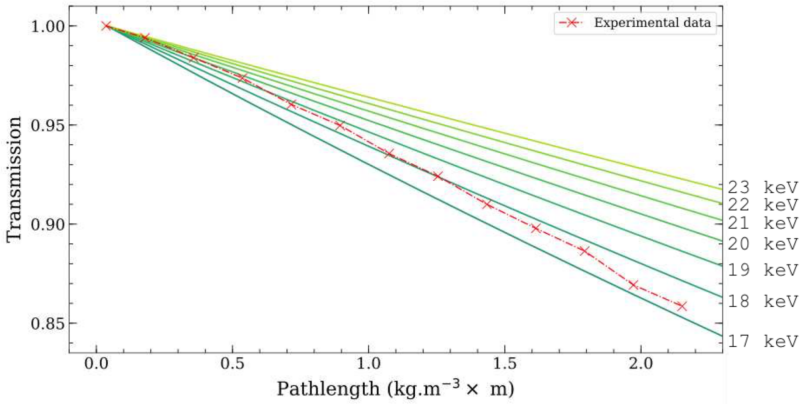

Figure 3: Calibration of the source X in the case of a chamber filled with nitrogen (at rest) experiencing various values of pressure. The transmission coefficient is normalized by its value at 0.1 MPa. Symbols: present source. Lines: theoretical values.

emitted and therefore the amount of X-rays. The high voltage between the anode and the cathode defines the shape of the Bremsstrahlung spectrum and the maximum energy of X-rays (E_{max}). In our case, a voltage of 25 kV is applies meaning that $E_{max} = 25$ KeV with a peak of X-rays emission [19] at $E_{max}/3 = 8$ keV.
Once emitted by the source, the X-rays beam crosses the fluid environment and hit a scintillator placed inside the chamber and linked to a camera operating in the visible spectrum. The scintillator Hamamatsu ACS J8734

(50×50 mm^2) is used with a luminescent layer of thallium doped cesium iodide, CsI (Tl). X-rays impacting the carbon plate yield an excitation that is transmitted to the CsI (Tl) layer, which produces a light intensity according to its excitation rate and the number of X-rays impacting the carbon plate. Such scintillator having an estimated efficiency of 70%, the effective transmission is then taken at 5 keV for the peak of X-rays emission, i.e. for subsequent calculations.

In order to characterize the source (configuration 25 kV and 0.5 mA), the X-ray transmission value (τ) is measured in the case of a chamber filled with nitrogen, at rest, and for different pressure values. In Fig. 3, the

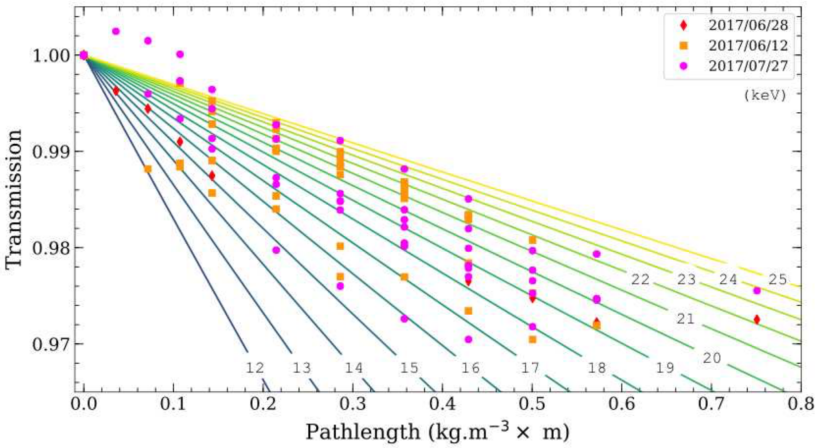

Figure 4: Calibration of the source X with various thicknesses of Kapton for the chamber windows, under atmospheric pressure. The transmission coefficient is normalized by its value without Kapton. Symbols: present source. Lines: theoretical values.

experimental value of the reduced transmission (τ^R), where $\tau^R = \tau/\tau_0$ with $\tau_0 = \tau|_{P=0.1\text{ MPa}}$, is plotted against the pathlength (i.e. density), and compared to theoretical values (see http://henke.lbl.gov for the X-rays database). The energy of X-rays is found between 17 keV and 23 keV. A second calibration is performed at atmospheric pressure with different thicknesses of Kapton for windows (from 25 to 525 μm). Three sets of measurements are performed to confirm the results. The resulting transmission coefficient is normalized by a reference case without Kapton. The results are compared to the theoretical transmission of Kapton as shown in Fig. 4. The energy of X-rays is found between 12 keV and 25 keV. It can be observed that for the thinnest thicknesses of Kapton, the reduced transmission coefficient is greater than one. This anomaly is attributed to the interaction between the target holder, that corresponds to a cylinder of 2 mm in aluminum.

Results and discussion

Shadowgraphy

A jet of Ethane discharging into an atmosphere of Nitrogen for a pressure chamber of 6.0 MPa is shown in Fig. 5 for different inlet velocities and two specific room temperatures. The structure of the jet is addressed by shadowgraphy and DBI, simultaneously. For a fixed temperature of 293 K for N_2 and C_2H_6, the sole influence of the inlet velocity is studied: for the highest velocities, $V_{inj} = 1.06$ m.s^{-1} and 2 m.s^{-1}, liquid atomization occurs and some droplets surround the jet. For $V_{inj} = 1.06$ m.s^{-1} the jet exhibits a second wind-induced regime whereas for $V_{inj} = 2$ m.s^{-1}, it is already an atomization mode [20]. Increasing the temperature of the chamber up to 323 K is higher than the critical temperature of ethane. On shadowgraphy images in Fig. 5 the structure of the jet seems similar whatever the temperature, but with a larger cone angle for a higher temperature. On DBI images, a clear modification of the jet topology is observed with temperature. Atomization efficiency is increased with temperature for the highest injection velocity. At $V_{inj} = 0.53$ m.s^{-1}, the interface becomes diffuse and a denser core is identifiable, but it is difficult to determine whether the structures around the jet are drops or not. The presence of liquid is questionnable. Finally, the diffuse topology of the jet at $V_{inj} = 0.27$ m.s^{-1} is close to a gaseous jet with no doubt about the absence of liquid. Under these conditions Ethane is injected under supercritical conditions.

Two topologic parameters are defined from shadowgraph images: the dark-core angle and the spreading angle also named growth rate [21]. From the normalized images of raw shadowgraphs, a two-level image is created. The black and white delimitation gives an interface between dense and light fluid. The calculation of the standard deviation of 120 two-level shadowgraph images yields the probability of presence of this interface on a grey-level

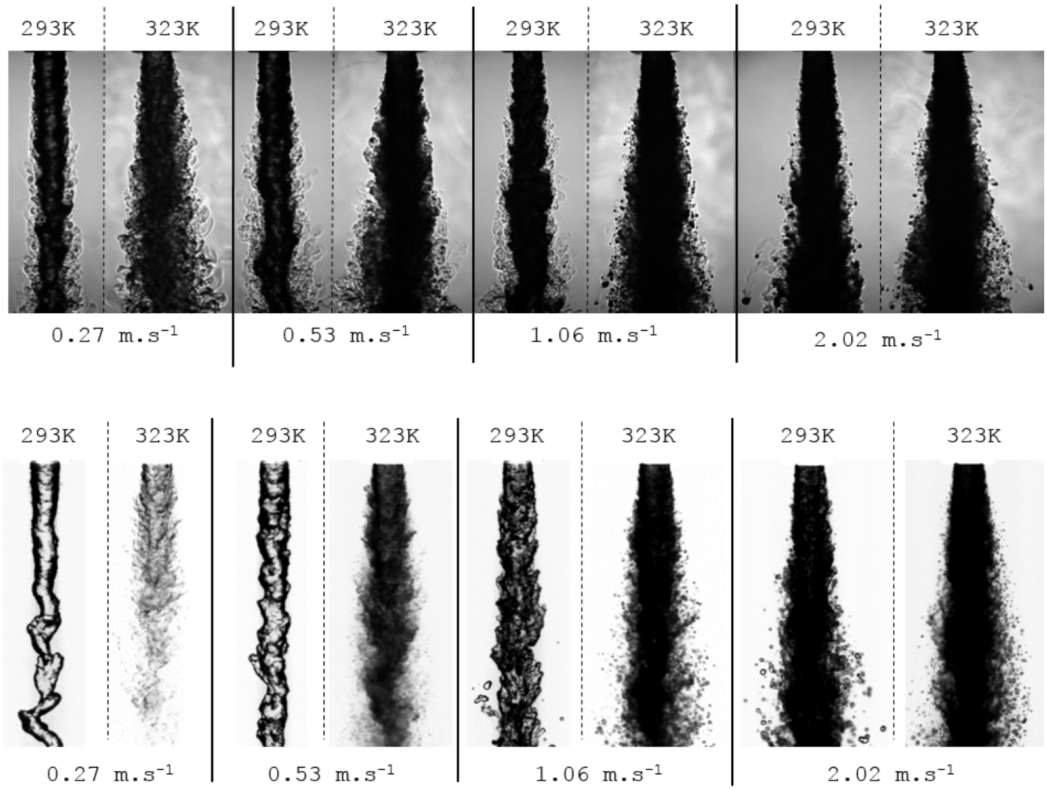

Figure 5: Jets of Ethane into Nitrogen at 6 MPa studied by shadowgraphy (top) and DBI (bottom). $T_{inj} = 293$ K and $V_{inj} = 0.27, 0.53, 1.06$ and 2.02 m.s^{-1}. $T_{ch} = 293$ K or 323 K.

scale. Only the values above 90 $\%$ of the maximum of this probability are retained to define the area delimited by the spreading angle θ_s that is located outside boundary. The spreading angle for different pressures, velocities and chamber temperatures of an Ethane jet in Nitrogen are plotted in Fig. 6.

To be compared to the results summarized by Chehroudi in [12], the spreading angle is plotted against the ambient over injectant density ratio. The density of pure fluids is based on the measured temperature and estimated from NIST tables. For each velocity, the growth rate increases with the pressure (also with the density ratio), which is in agreement with the other studies. At a given ambient pressure, the spreading angle increases with the velocity. Ethane spreading angles are smaller to the AFRL data for liquid N_2 in N_2 [12] having similar density ratios. This difference can be due to the velocity range in our experiments, which is one of the lowest in the literature but no indication of velocity is given on the original plot of Chehroudi (Fig. 8 in [12]). Increasing the temperature makes a significant change of flow topology at low velocities. In Fig. 6 (right), the injection of Ethane at $V = 0.25$ m.s^{-1} under a pressure of 5.0 MPa exhibits a density ratio of $\rho_{ch}/\rho_{jet} = 0.35$ contrary to configurations at higher pressure ($\rho_{ch}/\rho_{jet} \approx 0.20$). Indeed decreasing the pressure makes the working conditions closer to the critical point.

X-rays

The profiles of thickness density, Ep_ρ, are presently provided for the injections of Ethane into Helium at 5.5 MPa, the use of Nitrogen as surrounding fluid being not adapted to the technique of X-rays because of a weak transmission coefficient. Ep_ρ is calculated from average radiographic images as shown in Fig. 7 where an average, normalized and filtered image is obtained from 32 images of a jet at room temperature and $V_{inj} = 0.27$ m.s^{-1}. The shooting focuses on the first two openings of the window giving a field of 22 mm long. The nose of the injector can be seen in white on the left of the figure. The contours of the two openings are also discernible. It should be noted that gray level of these outlines on the normalized image suggests that X-rays are not totally blocked and interact with the edges of the openings. This interaction, probably geometric, could mean that X-rays are not totally parallel. The DBI images taken on the perpendicular axis during X-ray measurement are shown in Fig. 8 for $T_{ch} = 293$ K and Fig. 9 for $T_{ch} = 333$ K. The average of 120 DBI images of the jet at $V_{inj} = 0.27$ m.s^{-1} and $T_{ch} = 293$ K confirms that, in the vicinity of the nozzle outlet, the ethane jet thickness is 2 mm. Both DBI and X-rays images are consistent. Indeed, for each profile, a peak of energy is observed in the middle of the jet,

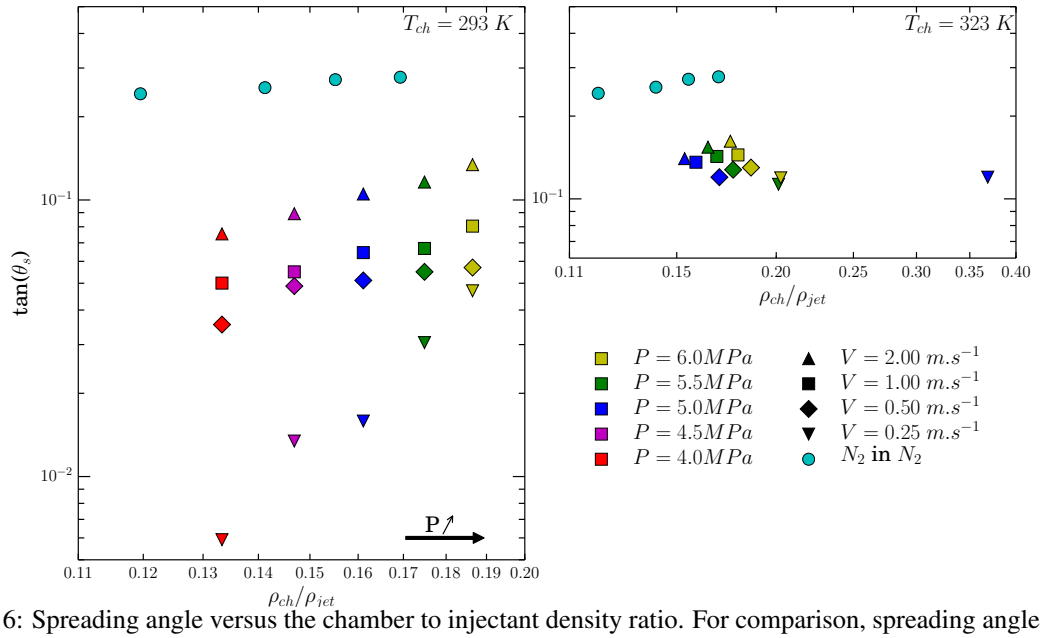

Figure 6: Spreading angle versus the chamber to injectant density ratio. For comparison, spreading angle of liquid N_2 injection in N_2 at ambient temperature from Fig. 8 of Chehroudi's paper [12].

Figure 7: Radiography (22 mm long) of a jet of Ethane into Helium at 5.5 MPa and $T_{ch} = 293$ K. $V_{inj} = 0.27$ m.s^{-1}.

i.e. at the point where the X-rays pass through the entire jet, before gradually decreases over the width of the jet because the jet is cylindrical on average. Moving away from the nose of the injector, the jet becomes thinner and the density of the thickness also decreases. The radial profiles of the thickness density is shown in Fig. 10.

Conclusions

A new fully instrumented experimental test-bench has been developed at CORIA lab to study the injection of inert fluids under supercritical conditions. In this study, Ethane is injected into a cold or warm environment of Nitrogen or Helium. The knowledge of the behavior of those fluids has been detailed. Results for the spreading angle are in agreement with the literature. It has been shown that the temperature of the ambient fluid played a major role in jet disintegration when pressure exceeds the critical pressure of the injected fluid. In case of an ambient temperature higher than the critical temperature of injected fluids a diffuse mixing process occurs for low discharge velocities. For a higher injection velocities, a process of atomization appears but with a larger spatial distribution of drops. These results were obtained by shadowgraphy and diffused backlight illumination that gave complementary information. The use of the X-rays technique to further characterize such jet has been proven in the case of Helium as surrounding fluid. A density measurement must still be refined but the first results are very encouraging.

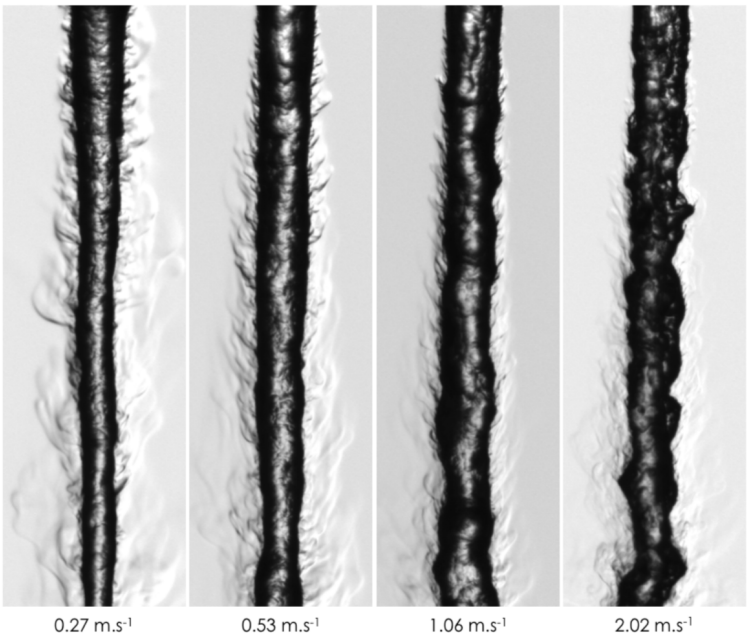

Figure 8: DBI (20 mm long) of a jet of Ethane into Helium at 5.5 MPa and $T_{ch} = 293$ K.

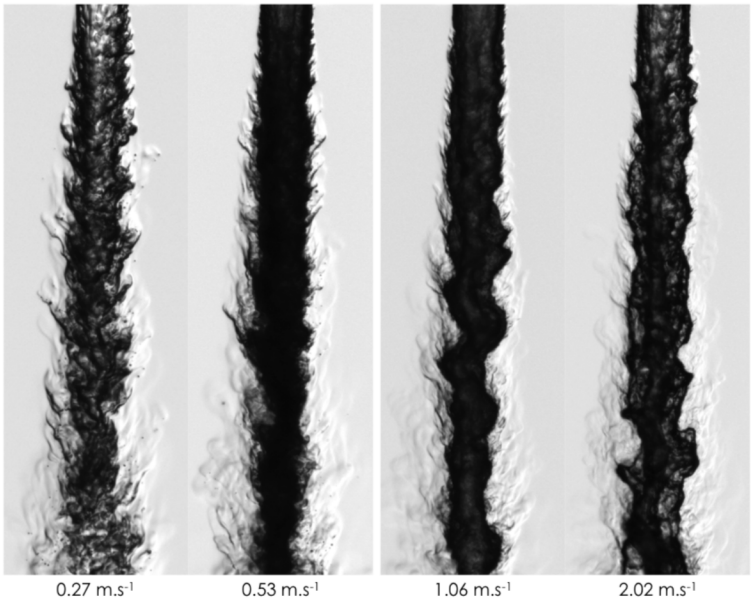

Figure 9: DBI (20 mm long) of a jet of Ethane into Helium at 5.5 MPa and $T_{ch} = 333$ K.

Acknowledgements

This work was funded by the ANR (Agence Nationale de la Recherche) research project REFINE (Real-gas Effects on Fluid Injection: a Numerical and Experimental study), Grant No. ANR-13-BS09-0007.

References

[1] R. Dahms, J. Oefelein. *Physics of Fluids*, 25(9):092103, 2013.
[2] R. Dahms, J. Oefelein. *Combustion and Flame*, 162(10):3648–3657, 2015.
[3] X. Petit, G. Ribert, G. Lartigue, P. Domingo. *The Journal of Supercritical Fluids*, 84:61–73, 2013.
[4] X. Petit, G. Ribert, P. Domingo. *The Journal of Supercritical Fluids*, 101:1–16, 2015.
[5] G. Ribert, X. Petit, P. Domingo. *The Journal of Supercritical Fluids*, 121:78–88, 2016.
[6] M. Oschwald, J. J. Smith, R. Branam, J. Hussong, A. Schik. *Combust. Sci. and Tech.*, 178:49–100, 2006.

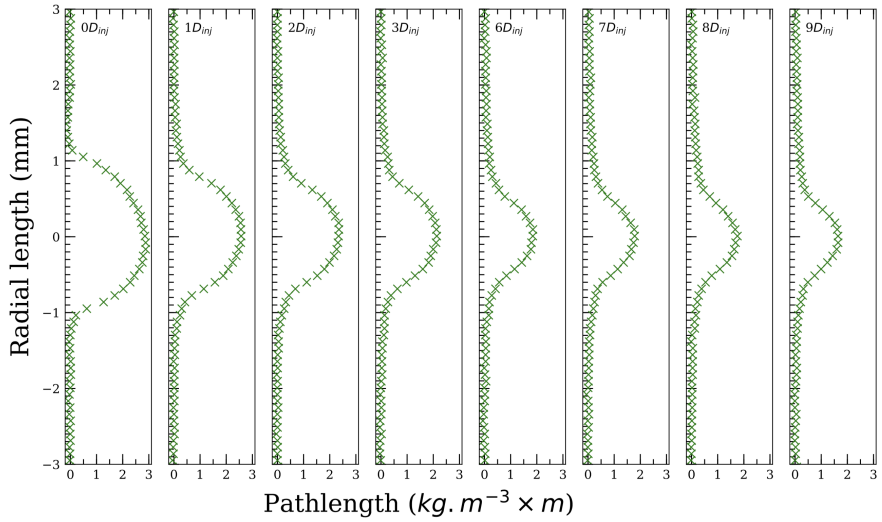

Figure 10: Radial profiles of the thickness density of a jet of Ethane at $V_{inj} = 0.27$ m/s in He at $P_{ch} = 5.5$ MPa and $T_{ch} = 293$ K at different distances from the injector expressed in nozzle diameter (D_{inj}). The energy of the source is considered at 8 keV.

[7] A. Cessou, O. Wequin, D. Stepowski. Alteration of the irradiance field when performing laser diagnostics in a corrugated liquid or supercritical jet. In *ILASS-Europe Zurich*, pages 561–567, (2001).

[8] J. Manin, M. Bardi, L. Pickett, R. Dahms, J. Oefelein. *Fuel*, 134:531–543, 2014.

[9] C. Segal, S. Polikhov. *Phys. Fluids*, 20:052101, 2008.

[10] W. Mayer, A. Schik, B. Vielle, C. Chauveau, I. Gokalp, D. Talley, R. Woodward. *Journal of Propulsion and Power*, 14(5):835–842, 1998.

[11] B. Chehroudi, D. Talley, R. Cohn. *Physics of Fluids*, 14-2:850–861, 2002.

[12] B Chehroudi, D Talley, W Mayer, R Branam, JJ Smith. Understanding injection into high pressure supercritical environments. Technical report, DTIC Document, 2003.

[13] W. Mayer, J. Telaar, R. Branam, G. Schneider, J. Hussong. *Heat and Mass Transfer*, 39:709–719, 2003.

[14] J. Manin, M. Bardi, L. Pickett, R. Payri. *International Journal of Multiphase Flow*, 83:267–278, 2016.

[15] J.-M. Pouvesle, C. Cachoncinlle, R. Viladrosa, E. Robert, A. Khacef. *Nuclear Instruments and Methods in Physics Research Section B : Beam Interactions with Materials and Atoms*, 113:134–140, 1996.

[16] E. Robert, S. Dozias, R. Viladrosa, C. Cachoncinlle, J.-M. Pouvesle. Table-top flash x-ray diagnostics of dodecane sprays. In *ILASS Europe*, 2010.

[17] B. Metay, E. Robert, R. Viladrosa, M. Dudemaine, C. Cachoncinlle, J.-M. Pouvesle, W. OH. Mayer, G. Scheinder, I. Gokalp. X-ray diagnostics applied to high pressure cryogenic sprays. In *9th ICLASS, Sorrento, Italy*, (2003).

[18] R. Behling. *Modern diagnostic X-ray sources : technology, manufacturing, reliability*. CRC Press, 2015.

[19] J. Bushberg, J. Boone. *The essential physics of medical imaging*. Lippincott Williams and Wilkins, 2011.

[20] C. Dumouchel. *Exp. Fluids*, 45:371–422, 2008.

[21] B. Chehroudi, R. Cohn, D. Talley. *Int. J. of Heat Fluid Flow*, 23:554–563, 2002.